Employing the lemma given in Ref. 14 and defining

$$Q_{k-1}{}^{\dagger} \triangleq E[w_{k-1}\, w_{k-1}{}^{T}] \tag{B5}$$

Eq. (B4) becomes

$$U_k = H(\bar{x}_k)[F(\hat{x}_{k-1})P_{k-1}F^{T}(\hat{x}_{k-1}) + Q_{k-1}{}^{\dagger} + C_{k-1}]H^{T}(\bar{x}_k) + R_k \tag{B6}$$

Comparing Eqs. (39) and (B6) yields

$$M_k{}^{\dagger} = F(\hat{x}_{k-1})P_{k-1}F^{T}(\hat{x}_{k-1}) + C_{k-1} + Q_{k-1}{}^{\dagger} \tag{B7}$$

Comparing Eq. (B7) to the unforced second-order filtering relation given in Eq. (31), one can see that the prior state error covariance matrix $M_k{}^{\dagger}$ contains the forcing matrix $Q_{k-1}{}^{\dagger}$ while in Eq. (31) the forcing matrix is missing. One may observe that if the same state estimate value of $\hat{x}_{k-1}$ is used for both methods, when the unknown thrusting is applied in the interval $[k-1, k]$, the rapid estimation scheme provides the correct state error covariance matrix while the second order filtering relation given in Eq. (31) provides an inaccurate estimate due to the presence of the unknown thrusting.

## References


[1] Swerling, P., "First Error Propagation in a Stagewise Smoothing Procedure for Satellite Observations," *Journal of the Astronautical Science*, Vol. 6, 1959, pp. 46–52.

[2] Gunckel, T. L., "Orbit Determination Using Kalman Method," *Proceedings of the Franklin Institute, Navigation*, Vol. 10(3), 1963, pp. 213–291.

[3] Rauch, H. E., "Optimum Estimation of Satellite Trajectories Including Random Fluctuations in Drag," *AIAA Journal*, Vol. 3, No. 4, April 1965, pp. 717–722.

[4] Shen, C. N., "Rapid Estimation of Covariance Matrices for Maneuvering Space Vehicle," AIAA Paper 70-1017, New York, 1970.

[5] Mowery, V. O., "Least Squares Recursive Differential Correction Estimation in Nonlinear Problems," *IEEE Transactions on Automatic Control*, Vol. AC-9, Oct. 1965, pp. 399–407.

[6] Kushner, H. J., "Dynamical Equations for Optimum Nonlinear Filtering," *Journal of Differential Equations*, Vol. 3, April 1967, pp. 179–190.

[7] Athans, M., Wishner, R. P., and Bertolini, A., "Suboptimal State Estimation for Continuous-Time Nonlinear System from Discrete Noisy Measurements," *IEEE Transactions on Automatic Control*, Vol. AC-13, No. 5, Oct. 1968, pp. 504–514.

[8] Battin, R., *Astronautical Guidance*, McGraw-Hill, New York, 1963.

[9] McClure, *Theory of Inertial Guidance*, McGraw-Hill, New York, 1961.

[10] Escobal, *Methods of Orbit Determination*, Wiley, New York, 1965.

[11] Mitchell, R. T., Reynolds, G. W., and Wang, S. K., "Use of Doppler Data to Monitor Space Craft Maneuvers," *JPL Space Programs Summary 37–57*, Vol. 11, 1970.

[12] Bryson, A. E. and Ho., Y. C., *Applied Optimal Control*, Ginn-Blaisdell, Waltham, Mass., 1969, Chap. 12.

[13] Sorenson, H. W., "Kalman Filtering Technique," *Advances on Control Systems*, edited by T. C. Leondes, Academic Press, New York, Vol. 3, A.C. 1966, pp. 219–292.

[14] Athans, M., Wishner, R. P., and Bertolini, A., "Suboptimal State Estimation for Continuous-Time Nonlinear Systems for Discrete Noisy Measurements," JACC Preprint, Ann Arbor, Mich., 1968, pp. 364–377.

[15] *IBM System-360 Programmer's Manual*, Scientific subroutine package, IBM (360A-CM-03X) version III, Feb. 1969.


JUNE 1972 AIAA JOURNAL VOL. 10, NO. 6

# An Analytical Model for Nitric Oxide Formation in a Gas Turbine Combustor

RICHARD ROBERTS,* LEONARD D. ACETO,† REINER KOLLRACK,‡ DONALD P. TEIXEIRA,§ AND JOHN M. BONNELL¶
*Pratt and Whitney Aircraft Division, United Aircraft Corporation, East Hartford, Conn.*

**An analytical model has been developed for predicting the influence of combustor geometry and operating conditions on nitric oxide emissions. The principal elements of the analysis are a three-zone internal flowfield model, a fuel droplet burning model incorporating either equilibrium or kinetic rate-limited hydrocarbon thermochemistry, and a treatment of the kinetics of nitric oxide formation. The postulated controlling mechanisms are incorporated using a numerical integration procedure coupled to the combustor flowfield. It is concluded that the assumption of equilibrium hydrocarbon chemistry is adequate for predicting nitric oxide concentration. Parametric results are presented indicating the influence of variation in primary zone equivalence ratio, combustor residence time, and initial fuel droplet size. The influence of a particular combustor modification is directly relatable to changes in the vapor-phase fuel-air distribution within the combustor.**

Presented as Paper 71-715 at the AIAA/SAE 7th Propulsion Joint Specialist Conference, Salt Lake City, Utah, June 14–18, 1971; submitted August 7, 1971; revision received January 27, 1972. The authors wish to acknowledge the assistance of B. C. Schlein.

Index categories: Combustion in Heterogeneous Media; Combustion in Gases; Reactive Flows.

* Assistant Project Engineer, Combustion T & R Group. Member AIAA.

† Assistant Project Engineer, Scientific Analysis Group. Member AIAA.

‡ Associate Research Scientist, Scientific Analysis Group.

§ Analytical Engineer, Combustion T & R Group; presently with Southern California Edison Company, Los Angeles, California.

¶ Senior Assistant Project Engineer, Combustion T & R Group. Member AIAA.

## Nomenclature

$A_{sw}$ = swirler flow area
$C_D$ = fuel droplet drag coefficient
$C_{pg}$ = specific heat of ambient gas
$C_{vsw}$ = swirler discharge coefficient
$D$ = fuel droplet diameter
$g$ = air mass flow rate through first combustion hole row
$i$ = stoichiometric oxygen-fuel weight ratio
$j$ = fraction of air upstream of the combustion holes entering the recirculation zone (referred to $g$)
$k$ = fraction of combustion hole air entering the recirculation zone (referred to $g$)
$K_i$ = ratio of one way equilibrium rate to net reaction rate
$k_i$ = reaction rate constant
$L$ = heat of vaporization of the fuel

$M_{ang}$ = axial flux of angular momentum leaving the swirler
$\dot{m}_f$ = rate of mass vaporization from droplet
$Pr$ = Prandtl number
$Q$ = heat of combustion of the fuel
$Re$ = Reynolds number
$R_i$ = one-way equilibrium rate
$R_r$ = ratio of recirculation zone boundary radius to combustor radius
$r_1$ = swirler inner radius
$r_2$ = swirler outer radius
$r_w$ = radius of combustor
$T_g$ = ambient gas temperature
$T_{in}$ = entry air jet temperature
$T_l$ = droplet surface temperature
$T_{pz}$ = average primary zone temperature
$U_g$ = absolute gas velocity
$U_d$ = droplet velocity
$V$ = axial volumetric flow rate
$v$ = airflow entering swirler (referred to $g$)
$Y_{O_2}$ = weight fraction of oxygen in ambient gas
$\alpha$ = ratio of kinetic to equilibrium NO concentrations
$\beta_0$ = angle of jet entry
$\theta$ = swirler vane turning angle
$\lambda_g$ = thermal conductivity of ambient gas
$\mu_g$ = viscosity of the ambient gas
$\rho_f$ = fuel liquid density
$\rho_g$ = ambient gas density

## Introduction

ALTHOUGH it is recognized that exhaust emissions from aircraft gas turbines constitute a relatively minor source of atmospheric pollution,[1] work is in progress to investigate possible means for reducing emission levels. The earliest work concerned itself with visible emissions and resulted in the development of combustor design techniques for reducing exhaust smoke emission below the level of visibility.[2] More recent efforts have been directed towards reducing high-power nitrogen oxide emissions, particularly from ground-based industrial engines. These emissions are produced at the high combustion temperature required for maximum engine power, and are potentially the most difficult of the emissions to control. The most obvious means of control is to reduce the peak combustion temperature. To accomplish this while satisfying other engine requirements will require significant combustion chamber modification and may incur a penalty in engine performance. In an effort to simultaneously consider the competing high performance and low emissions requirements, and to reduce the amount of testing required, emphasis has been given to the development of an analytical model for nitric oxide formation in a gas turbine combustion chamber.

Experimental values of exhaust gas nitric oxide concentration are available for a variety of gas turbine engines.[3-5] By comparing these measurements with equilibrium levels corresponding to local gas temperatures, Marteney,[6] Heywood et al.,[7] and others have shown that the nitric oxide formation reactions do not proceed to equilibrium. Nitric oxide formation is kinetic rate limited in the high-temperature regions of the combustion chamber, with the reactions being frozen by the addition of dilution air before equilibrium is reached, Once formed, the nitric oxide concentration is reduced only by dilution. Essentially the same conclusion was reached by Sawyer et al.[8] from examination of probing data taken in a laboratory combustor.

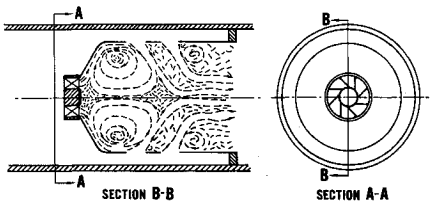


**Fig. 1 Primary zone flow pattern observed in a can-type combustion chamber.[9]**

Thus, to accurately predict the rate of nitric oxide emission from a gas turbine engine, it is necessary to take into account the principal physical and chemical mechanisms which influence its formation. These mechanisms are influenced by combustor gas temperature, chemical species concentrations, and residence time as primary variables. These variables are in turn influenced by engine operating conditions, details of the combustor internal flowfield, fuel spray characteristics, and the rate of air addition.

## Approach to Combustor Modeling

The approach taken in this study is to develop mathematical treatments for postulated physical and chemical rate-controlling mechanisms and to integrate these mechanisms through a sequence of thermodynamic states obtained from the coupling between these mechanisms and the physical combustor flowfield. The simultaneous solution of the combustion rate mechanisms and the fluid dynamics provides the gas temperature, flow velocity, and chemical species concentrations as a function of position within the combustor. These flow conditions and species concentrations influence nitric oxide concentration through the mechanism for its formation. The principal elements of the analysis are a combustor internal flowfield model, a fuel droplet dynamics and vaporization model, a combustion heat release model, and a treatment of finite-rate nitrogen-oxygen kinetics.

Since a primary objective of the model is to assist in the development of a reduced nitric oxide combustor configuration, the analysis must include sufficient detail such that a correspondence can be drawn between nitric oxide emissions and combustor geometry, fuel injection characteristics, and engine operating conditions. The treatment of individual submodels allows a reasonable amount of detail to be incorporated in a tractable mathematical analysis. The scope of this study has been confined to conventional swirl-stabilized combustor designs with axial injection of liquid fuel. Since the model employs a combination of one-dimensional flow analyses and places principal emphasis on the primary combustion zone, it may be applied equally well to a can-type combustor or a single-swirler sector of an annular combustor.

## Description of Combustor Model

### Internal Flowfield Model

The combustor flowfield model, with input quantities of chamber area vs axial distance, inlet air temperature, chamber pressure, and axial location of air entry holes, provides the physical quantities upon which the gas dynamic and chemical rate calculations are based. The experimentally determined internal flowfield for a conventional can-type combustor is shown in Fig. 1. The flowfield is divided into a region of highly turbulent recirculating flow in the front of the chamber followed by a region of relatively uniform downstream flow. The forward reversed flow region is designated the primary zone and the downstream region the secondary or dilution zone. The division occurs at the first row of liner penetration jet holes. The primary zone serves the purpose of stabilizing the combustion process. The liquid fuel is

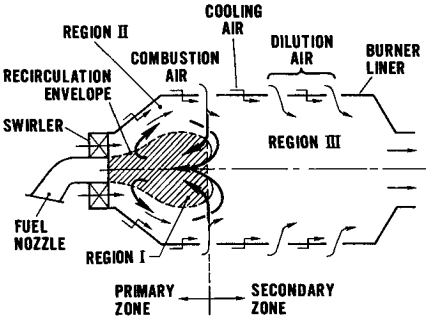


**Fig. 2 Schematic of internal flowfield model.**

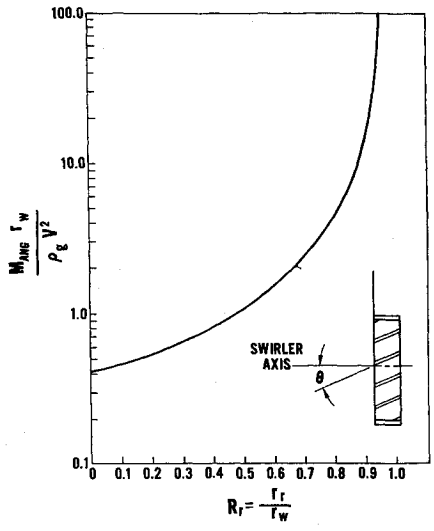


**Fig. 3 Recirculation core radius function.**[11]

conditioned for burning and combustion is largely completed in this zone. The mixture of high-temperature combustion products and reactants leaving the primary zone is burned to completion and subsequently mixed with dilution air in the secondary zone to provide a suitable temperature level and profile for entrance to the turbine.

The combustor flowfield model employed in the present analysis is shown schematically in Fig. 2. The primary zone consists of a central recirculation zone (region I), characterized by reversed flow and high levels of turbulence and temperature, and an outer streamtube of reacting flow (region II). The dilution zone (region III) is modeled as a single streamtube in which chemical reaction may occur. By considering the primary zone to be divided into two parallel flow paths, a combination of one-dimensional analyses is used to represent the salient two-dimensional features. The airflow distribution to the swirler, primary and secondary combustor holes, and cooling holes is determined by means of a calculation procedure similar to that reported in Ref. 10. This calculation procedure is capable of treating effects due to heat addition, variation in the discharge coefficient of air entry holes, and axial variation of liner pressure drop. In keeping with the one-dimensional nature of the flowfield treatment, air added to the combustor through liner holes is assumed to mix instantaneously with the internal flow.

The recirculation zone boundary is determined by use of the semiempirical correlation of Ref. 11

$$R_r = f[M_{\text{ang}} r_w/\rho_g V^2] \tag{1}$$

The functional relationship of Eq. (1) has been developed in Ref. 11 (see Fig. 3). The independent parameter $M_{\text{ang}} r_w/\rho_g V^2$ may be expressed in terms of geometric parameters as follows:

$$M_{\text{ang}} r_w/\rho_g V^2 = (2\pi r_w/3A_{sw}{}^2 C_{vsw}) \tan\theta [r_2{}^3 - r_1{}^3] \tag{2}$$

Once the recirculation region has been defined, the area between its boundary and the chamber wall defines the streamtube region (region II).

It is assumed that unburned air enters the recirculation region (region I) only by entrainment from the combustion-air jets at the downstream boundary of the primary zone. The quantity of air entering the upstream flow region is determined through application of an empirical correlation[12] derived primarily from the experimental results of Rosenthal.[13] With reference to the flow model of Fig. 4, the fraction of combustion jet air ($k$) entering the recirculation zone is given by

$$k = 0.5\,[T_{\text{in}}/T_{pz}]^{1/2} \cos\beta_0 \tag{3}$$

An additional quantity of upstream fuel-air-combustion product mixture enters region I from region II. Entrainment in the combustion air jets is the principal mechanism for this recirculation. This quantity of flow, designated $j.g$ in Fig. 4, is assumed to be equal in magnitude to the recirculation flow from the combustion holes $k.g$. All flow recirculating upstream in region I is assumed to enter region II at the swirler face. The combustion products from region I are assumed to mix instantaneously with the unburned air entering region II. Other than these discrete input flow adjustments to account for mass transfer between regions, there is no interaction between the primary zone flow regions.

### Fuel Droplet Vaporization

The total combustor fuel flow is divided between regions I and II in the ratio of the recirculation region gas flow, $j.g$, to the total region II flow, on the assumption that similar entrainment mechanisms are responsible. The flow in region I is highly turbulent with a residence time which is long compared to the hydrocarbon chemical relaxation time. Fuel which enters region I is assumed to be fully vaporized and perfectly mixed with the region I airflow. The combustion of fuel is also assumed to be instantaneous in this region. The rate-controlled nitric oxide chemistry then proceeds at the final flame temperature for a residence time equal to the volume of region I divided by the volumetric flow rate. The flow in region II is modeled as a one-dimensional reacting streamtube with the combustion process governed by the rate of fuel droplet vaporization in the presence of diffusive burning. It is assumed that the fuel spray is uniformly distributed across the region II streamtube, that interaction between burning droplets is insignificant, that vaporized fuel mixes instantaneously with the surrounding gas phase mixture, and that the spray can be adequately characterized by a single value of Sauter Mean Diameter (SMD).

The fuel droplet vaporization rate in region II is calculated from the following expression due to Wood, Lorell, Rosser, and Wise[14,15]:

$$\dot{m}_f = (2\pi D\lambda_g/C_{pg}) \ln [1 + QY_{O_2}/Li - (C_{pg}/L)(T_l - T_g)] \tag{4}$$

Equation (4) is based on assumptions of spherical symmetry, steady-state conditions, transport properties are not temperature or composition dependent, and negligible radiation effects. An analysis, employing the model developed in Ref. 16, has shown that for typical gas turbine engine operating conditions the droplet transient temperature period is negligible compared to the steady-state burning period. Therefore, the liquid surface temperature is assumed equal to the boiling point. Equation (4) was developed for a droplet burning in a quiescent atmosphere, and therefore does not take into account the effects of convective mass transport. Equation (4) is multiplied by

$$1.0 + 0.276\, Re^{1/2}\, Pr^{1/3}$$

where the Reynolds number is given by

$$Re = |U_g - U_d|\, D\rho_g/\mu_g$$

and the Prandtl number by

$$Pr = C_{pg}\mu_g/\lambda_g$$

to account for convection.[17]

Since the droplet velocity typically differs from that of the gas, acceleration or deceleration of the droplet due to viscous drag must be included. This is accomplished by including a drag force term in the droplet momentum equation. The resulting differential equation for droplet velocity is

$$dU_d/dt = (3C_B \rho_g/4D\rho_f)|U_g - U_d| \cdot (U_g - U_d) \tag{5}$$

The drag coefficient is calculated from one of the following equations, depending on Reynolds number[18]:

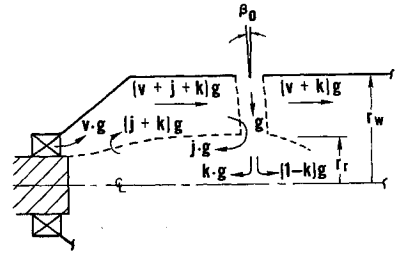


**Fig. 4 Combustor primary zone airflow distribution.**

**Table 1 Hydrocarbon oxidation kinetics system**

| Reaction | Forward rate constant, $cm^3$/mole-sec | |
|---|---|---|
| $C_8H_{16}+O_2 = 2C_4H_8O$ | $k_1 = 5\times10^7\, T^{1.5}\, e^{-7900/T}$ | (a) |
| $2C_4H_8O+3O_2 = 8CO+8H_2$ | $k_2 = 1\times10^{11}\, T^{4.5}$ | (a) |
| $O+H_2O = 2OH$ | $k_3 = 5.75\times10^{13}\, e^{-9000/T}$ | (b) |
| $2H+M = H_2+M$ | $k_4 = 2\times10^{18}\, T^{-1}$ | (c) |
| $2O+M = O_2+M$ | $k_5 = 1\times10^{17}\, T^{-1}$ | (d) |
| $OH+H+M = H_2O+M$ | $k_6 = 7\times10^{19}\, T^{-1}$ | (e) |
| $H+O_2 = OH+O$ | $k_7 = 2.24\times10^{14}\, e^{-8400/T}$ | (b) |
| $O+H_2 = OH+H$ | $k_8 = 1.74\times10^{13}\, e^{-4730/T}$ | (b) |
| $CO+OH = CO_2+H$ | $k_9 = 5.6\times10^{11}\, e^{-540/T}$ | (b) |
| $H+H_2O = OH+H_2$ | $k_{10} = 8.41\times10^{13}\, e^{-10050/T}$ | (b) |

[a] These are arbitrary global rates adjusted to fit experimental ignition delay data following the approach taken in Ref. 23.
[b] Ref. 24.
[c] Ref. 23.
[d] Average of rates presented in Refs. 26 and 27, adjusted for a $T^{-1}$ temperature dependency as given in Ref. 25.
[e] Average of rates presented in Refs. 23 and 24, adjusted for a $T^{-1}$ temperature dependency as given in Ref. 25.

$$C_D = 27\,Re^{-0.84} \qquad 0 < Re \leqq 80$$
$$C_D = 0.271\,Re^{0.217} \quad 80 < Re \leqq 10^4; \quad C_D = 2.0 \quad 10^4 < Re \tag{6}$$

The initial conditions of mean drop size and injection velocity are a function of nozzle characteristics. The SMD is employed to describe the coarseness of the fuel spray and is calculated from empirical correlations for the type of nozzle employed. Consistent with the assumption of a single droplet diameter, a uniform droplet injection velocity is estimated using the orifice discharge equation. The droplet velocity is assumed to be parallel to the region II streamtube axis. Values of surface tension, heat of vaporization, viscosity, specific gravity and heat of combustion for JP-5 fuel are taken from Ref. 19. The liquid drop temperature, $T_l$ is taken to be the ASTM 50% distillation point in accordance with the conclusions reached in Ref. 15 for multicomponent fuel blends.

### Hydrocarbon Thermochemistry

The quantity of fuel vapor obtained from Eq. (4) in an increment of burner length, when mixed with the pre-existing vapor fuel-air-combustion product mixture at that axial station, is available for combustion. Chemical reaction of the hydrocarbon fuel and air determines the gas temperature and concentration of active combustion species. In developing an analysis of nitric oxide formation there is good basis for assuming that the hydrocarbon chemistry may be decoupled from the nitric oxide chemistry. This is due to the fact that the nitrogen-oxygen chemistry is slow compared to the hydrocarbon combustion rate, as shown by Marteney.[6] This assumption permits the use of an equilibrium hydrocarbon thermochemistry model. Application of this model results in instantaneous combustion of the vapor-phase fuel-air mixture and provides equilibrium concentrations of O, OH, N, etc., as input to the nitric oxide formation kinetics. However, Bowman[20] has pointed out that under some circumstances, O-atom and N-atom concentrations can overshoot the equilibrium values by significant amounts. The validity of the decoupling assumption was investigated in the present study by including a simultaneous treatment of hydrocarbon oxidation kinetics with the nitric oxide formation kinetics. Results obtained from this calculation are compared with the corresponding uncoupled-equilibrium heat release case. The calculation subroutine employed for the equilibrium hydrocarbon thermochemistry is based on procedures due to Brinkley.[21,22]

The kinetics of hydrocarbon fuel breakdown include cracking reactions, peroxides forming reactions and radical-attack reactions. The number of reactions involved is extremely large, and few have been investigated with respect to their rates. It is, therefore, convenient to consider the fuel breakdown to elemental species in a single global step. The hydrocarbon kinetic system employed in the present study is described in Table 1. It follows the pattern of the quasi-global system presented by Edelman and Fortune.[23] The referenced system was modified by introducing the hypothetical aldehyde intermediate ($C_4H_8O$) for reasons of compatibility with the available chemical kinetics computer program. Since it is a short-lived intermediate, the effect is a negligible transitory one. In addition, the O+H recombination reaction involving a general third body has been eliminated since it was found to be of negligible importance. The rate constants are taken from Refs. 23 to 27 as indicated in Table 1. The global rates have been adjusted to fit experimental ignition delay data following the outline of Ref. 23. JP-5 fuel is represented by $C_8H_{16}$, although it is not meant to be an olefin. Its thermodynamic properties (specific heat, heat of formation) are consistent with the fuel. The chemical kinetics computer program employed in this study was developed by one of the authors and later used by Marteney.[6]

The full kinetic system, including both hydrocarbon and nitric oxide chemistry, is utilized only in regions II and III in conjunction with the droplet vaporization equations. The nature of the flow in region I is such that the assumption of instantaneous equilibrium heat release is justified.

**Table 2 Nitric oxide formation kinetics[a]**

| Reaction | Forward rate constant, $cm^3$/mole-sec |
|---|---|
| $N+NO = N_2+O$ | $k_{11} = 1.2\times10^{-13}$ |
| $N+O_2 = NO+O$ | $k_{12} = 1.2\times10^{13}\, e^{-3575/T}$ |
| $N+OH = NO+H$ | $k_{13} = 4.22\times10^{13}$ |
| $H+N_2O = N_2+OH$ | $k_{14} = 3.01\times10^{13}\, e^{-5438/T}$ |
| $O+N_2O = N_2+O_2$ | $k_{15} = 3.61\times10^{13}\, e^{-12084/T}$ |
| $O+N_2O = NO+NO$ | $k_{16} = 4.82\times10^{13}\, e^{-12084/T}$ |

[a] Ref. 28.

### Nitric Oxide Formation

The nitric oxide formation system described in Table 2 is due to Lavoie et al.[28] These six reactions are added to the hydrocarbon oxidation reactions and are included in the simultaneous solution of the set of rate equations. The nitric oxide formation reactions may thus be influenced by nonequilibrium levels of active combustion species.

In the case of the equilibrium heat release model, concentrations of O, $O_2$, H, OH, and $N_2$ are assumed to be the local equilibrium values. This allows expressions to be written for the rate of change of the concentrations of NO, N, and $N_2O$. A further assumption that the concentrations of N and $N_2O$ are at steady-state permits the derivation of the following rate equation[28]:

$$d[NO]/dt = 2(1-\alpha^2)[R_{11}/(1+\alpha K_1)+R_{16}/(1+K_2)] \tag{7}$$

where

$K_1 = R_{11}/(R_{12}+R_{13})$; $K_2 = R_{16}/(R_{14}+R_{15})$; $\alpha = [NO]/[NO]_e$

$R_i$ is the one-way equilibrium rate of the $i$th reaction, for example,

$$R_{11} = k_{11}[N]_e[NO]_e$$

### Computational Procedures

The calculation is started by specifying the fuel and air flow distributions. The external airflow addition rates are determined from the combustor geometry and liner pressure drop. The internal airflow distribution is determined by application of the entrainment calculation procedure described above. The fuel flow is divided among regions I and II in proportion to the ratio of recirculating region II gas flow to total region II flow.

The nitric oxide calculation begins with region I. The region I equivalence ratio is obtained by algebraic manipulation of the input fuel and airflow rates. The region I gas temperature follows from the mixture ratio and the compressor discharge temperature, pressure and fuel type. The concentration of nitric

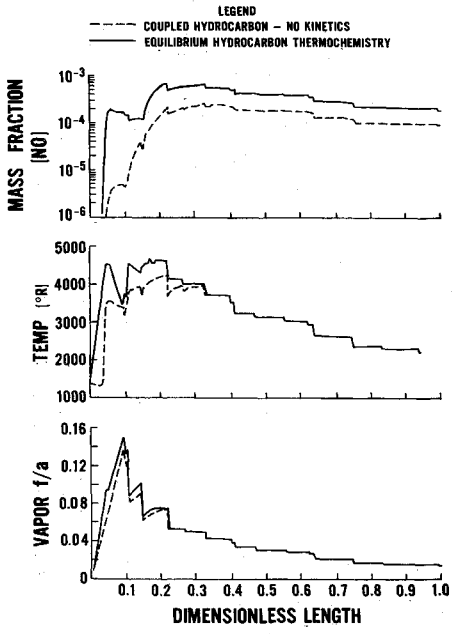


**Fig. 5 Comparison of coupled hydrocarbon: nitric oxide kinetics and uncoupled equilibrium hydrocarbon: nitric oxide kinetics systems.**

oxide formed in region I is then calculated from Eq. (7), using the equilibrium combustion species concentrations and the region I mean residence time.

The flow leaving region I is mixed instantaneously with the region II inlet airflow at the swirler face on an enthalpy basis. This provides an initial concentration of combustion products (expressed as a previously reacted vapor-phase fuel-air ratio), and an increased inlet temperature, which act to accelerate the droplet vaporization and chemical reaction processes. The simultaneous droplet vaporization and chemical kinetics calculation is initiated at this point and solved using an iterative technique. The convergence criteria and step size necessary for accurate results have been established through experience. The transition from region II to region III is continuous. Any fuel which is unvaporized or unburned will continue to react in the region III streamtube.

An initial nitric oxide concentration of zero is presently used to start the region I calculation. In reality, a quantity of nitric oxide is entrained from region II. However, since the mixture in region I is typically fuel-rich, this level will pass through the region virtually unchanged. Likewise, in region II, once an appreciable level of NO is obtained the rate of formation is

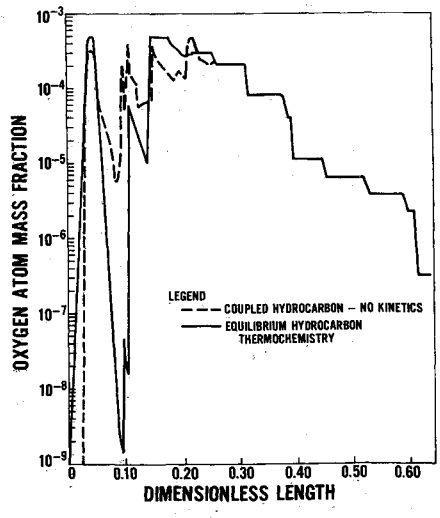


**Fig. 6 Comparison of equilibrium and nonequilibrium oxygen atom concentration.**

reduced and becomes O concentration limited. Thus the assumption of zero initial nitric oxide concentration entering the recirculation zone is adequate within the context of this model.

## Results

The flowfield model and calculation procedures described in the previous section have been programed for solution on a digital computer. The calculation produces detailed information concerning fuel droplet size, droplet velocity, gas velocity, vaporized fuel-air ratio, gas temperature, hydrocarbon combustion product species concentrations, and nitric oxide concentration as a function of axial length. The program additionally provides the fuel-air ratio, gas temperature and nitric oxide concentration produced in region I, as well as the cumulative residence time for regions I, II, and III. The combustor dimensions, fuel spray characteristics, and airflow distribution used in this study are typical of can-type, single nozzle combustors currently in service. Parametric variations about this baseline configuration were investigated to determine the sensitivity of nitric oxide formation to particular combustor modifications.

Results obtained from the coupled hydrocarbon-nitric oxide kinetic system for a plug flow combustor burning liquid fuel are shown in Fig. 5. A comparison is made with results obtained from the uncoupled equilibrium heat release-nitric oxide kinetic system. The temperature response and droplet vaporization behavior predicted by the coupled system are in qualitative agreement with available experimental results.[8] The equilibrium and nonequilibrium oxygen atom concentrations are compared in Fig. 6. It can be seen from Fig. 6 that the oxygen atom concentration briefly exceeds the corresponding equilibrium value in the region of peak heat release, by a considerable amount. The kinetic flame temperature, however, remains below the equilibrium values. The net effect of employing the full kinetic system, as shown in Fig. 5, is to predict nitric oxide concentration a factor of two below that obtained from the equilibrium combustion system. There are significant differences in the early part of the combustor attributable to ignition delay time. These differences would be minimized when the products of region I combustion preheat the region II input flow. It may be concluded that the results obtained from the two calculation schemes are essentially similar, and that the assumption of equilibrium hydrocarbon chemistry is adequate for the present model. Use of the equilibrium hydrocarbon system affords considerable computational simplification.

The results which follow were obtained using the three-zone combustor model with equilibrium heat release and nitric oxide formation governed by Eq. (7). Figures 7–9 show predicted results obtained from variation of several combustor design parameters. These are primary zone fuel-air ratio, combustor residence time, and initial fuel droplet size. In Fig. 7, axial distributions of vapor-phase fuel-air ratio, gas temperature and nitric oxide concentration are shown for the baseline combustor and two cases where the primary zone air admission rate is 20% higher and 20% lower than the baseline. This airflow variation produces approximately the same variation in vapor-phase mixture conditions. Nitric oxide formed in region I appears in Figs. 7–9 as an initial concentration at the front of the combustor. Both airflow variations result in a small decrease in nitric oxide concentration. Nitric oxide formation is quenched somewhat earlier in the leaner primary zone and considerably later in the fuel-rich case.

Figure 8 presents results obtained by varying the combustor residence time. Configurations having a 50% longer primary zone and a 50% longer dilution zone are compared with the baseline. These variations were obtained by axially expanding the baseline airflow distribution. Increasing primary zone length has a minimal effect on final nitric oxide concentration, largely due to the fuel rich mixture conditions. Lengthening the dilution zone, however, results in a greater level of nitric oxide due to longer residence time before quenching by dilution air addition.

Figure 9 shows the predicted effects due to changes in fuel droplet size. Cases having twice and one-half the baseline SMD

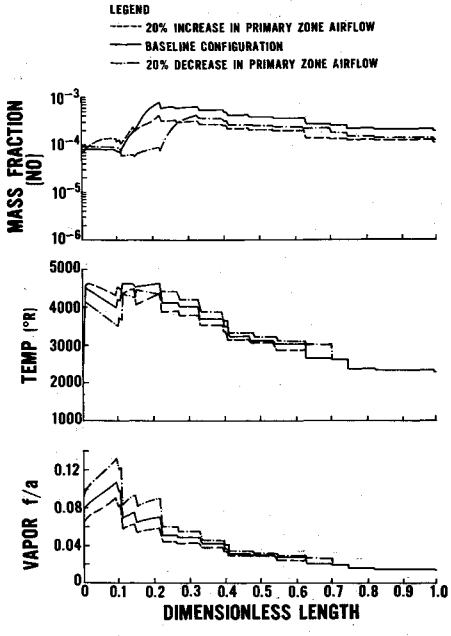


Fig. 7 Effect of primary zone fuel-air ratio.

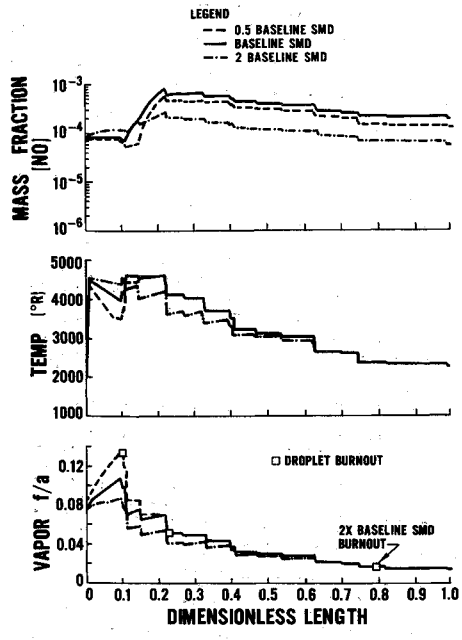


Fig. 9 Effect of initial fuel droplet size.

are shown. Since vaporization rate is dependent on droplet surface to volume ratio, changes in droplet size have a strong influence on vapor-phase mixture conditions for a given airflow distribution. As shown in the figure, both cases reduced the final nitric oxide concentration. The smaller droplet vaporizes quickly and produces a very rich primary zone mixture, while the larger droplet vaporizes slowly and produces a quite lean fuel-air distribution.

The absolute values of nitric oxide concentration predicted by the model (100–200 ppmw) are in reasonable agreement with available experimental data measured at the engine discharge.[5] It can be seen from Figs. 7–9 that the extent to which a particular configuration change affects nitric oxide concentration depends directly on the corresponding change in local mixture conditions. The results indicate that there are two principal sites of nitric oxide formation in a conventional gas turbine combustor. The first of these is the reversed-flow recirculation zone (region I). Although mixture conditions are generally fuel rich, the residence time in this zone is relatively long. The second significant region of nitric oxide formation is in the upstream end of region III, where the local gas mixture passes from fuel-rich primary zone conditions to fuel-lean dilution zone conditions. The quantity of nitric oxide produced is proportional to the residence time at peak temperature conditions. The formation of nitric oxide abruptly ceases as the gas temperature falls below 3600–3800°R. From that point on, nitric oxide concentration is reduced only by the addition of dilution air.

A number of cases presented in Figs. 7–9 show a net reduction in nitric oxide concentration over the baseline configuration. Unfortunately, the real life situation is complicated by numerous combustor performance requirements which are readily compromised by the type of modification discussed here. For example, in Fig. 9 the smaller droplet burns out quickly but produces a primary zone fuel-air mixture well in the range of smoke formation. On the other hand, the larger droplet does not burn out until near the end of the combustor, presenting potential turbine durability problems. Thus the trends obtained from a parametric investigation of the type presented here must be considered only as potential directions to follow until all combustor performance requirements can be simultaneously satisfied. A general discussion of the characteristics required for acceptable over-all combustor performance is beyond the intent of this paper.

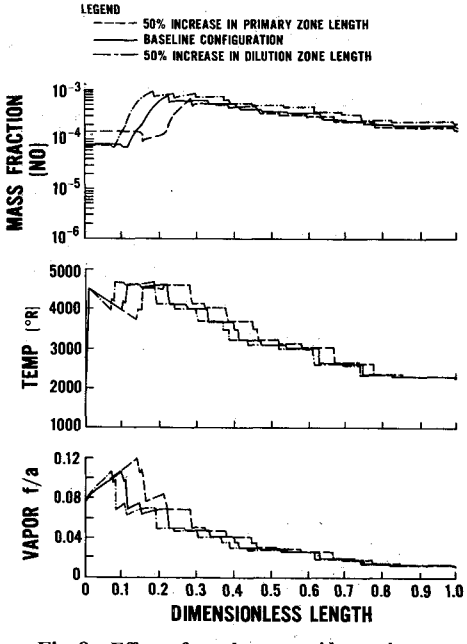


Fig. 8 Effect of combustor residence time.

## Conclusions

The three-zone combustor model developed in this study has been shown to predict absolute levels of nitric oxide concentration which are in general agreement with available experimental data. In addition, the predicted nitric oxide concentration is sensitive to variations in combustor geometry, fuel injection characteristics and engine operating conditions, in direct relation to the vapor-phase fuel-air mixture distribution within the combustor. For these reasons, it is concluded that the present modeling approach provides a useful means of identifying the significant features which influence nitric oxide formation in a gas turbine combustion chamber and of assessing the nitric oxide emission characteristics of proposed combustor configurations.

Comparison of the coupled and uncoupled hydrocarbon thermochemistry systems for conditions typical of gas turbine combustion chambers indicates that both systems predict essentially the same final nitric oxide concentration. It is therefore, concluded that the hydrocarbon chemistry can be decoupled

from the kinetics of nitric oxide formation in the context of the modeling approach employed in this study.

## References

[1] Bastress, E. K. and Fletcher, R. S., "Aircraft Engine Exhaust Emissions," ASME Paper 69-WA/APC-4, Los Angeles, Calif., 1969.

[2] Faitani, J. J., "Smoke Reduction in Jet Engines Through Burner Design," SAE Paper 680348, New York, 1968.

[3] Smith, D. S., Sawyer, R. F., and Starkman, E. S., "Oxides of Nitrogen from Gas Turbines," *Journal of the Air Pollution Control Association*, Vol. 18, 1968, pp. 30–35.

[4] Lozano, E. R., Melvin, W. W., and Hochheiser, S., "Air Pollution Emissions from Jet Engines," *Journal of the Air Pollution Control Association*, Vol. 18, 1968, pp. 392–394.

[5] Bristol, C. W., "Gas Turbine Engine Emission Characteristics and Future Outlook," *Proceedings of the SAE/DOT Conference on Aircraft and the Environment*, Pt. I (P-37), 1971, pp. 84–92.

[6] Marteney, P. J., "Analytical Study of the Kinetics of Formation of Nitrogen Oxide in Hydrocarbon-Air Combustion," *Combustion Science and Technology*, Vol. 1, 1970, pp. 461–469.

[7] Heywood, J. B., Fay, J. A., and Linden, L. H., "Jet Aircraft Air Pollutant Production and Dispersion," AIAA Paper 70-115, New York, 1970.

[8] Starkman, E. S., Mizutani, Y., Sawyer, R. F., and Teixeira, D. P., "The Role of Chemistry in Gas Turbine Emissions," ASME Paper 70-GT-81, Brussels, Belgium, 1970.

[9] Clarke, J. S., "The Relation of Specific Heat Release to Pressure Drop in Aero-gas-turbine Combustion Chambers," *Proceedings of the 1955 IME-ASME Conference on Combustion*, 1955, pp. 354–361.

[10] Tacina, R. R. and Grobman, J., "An Analysis of Total Pressure Loss and Airflow Distribution for Annular Gas Turbine Combustors," TN D-5385, Aug. 1969, NASA.

[11] Kind, C. and Youssef, T., "Calculating the Flow in the Combustion Chamber of Gas Turbines," *Brown Boveri Review*, Vol. 51, 1964, pp. 808–816.

[12] "Computer Program for the Analysis of Annular Combustors, Volume I: Calculational Procedures," Rept. 1111-1, 1968, Northern Research and Engineering Corp., Cambridge, Mass.

[13] Rosenthal, J., "Exploratory Methods for the Determination of Gas Flow and Temperature Patterns in Gas Turbine Combustors," Mech. Eng. Note 235, 1959, Aeronautical Research Lab., Dept. of Supply, Australia.

[14] Wise, H., Lorell, J., and Wood, B. J., "The Effects of Chemical and Physical Parameters on the Burning Rate of a Liquid Droplet," *Fifth Symposium (International) on Combustion*, The Combustion Inst., 1955, pp. 132–141.

[15] Wood, B. J., Rosser, W. A., and Wise, H., "Combustion of Fuel Droplets," *AIAA Journal*, Vol. 1, No. 5, May 1963, pp. 1076–1081.

[16] Priem, R. J. and Heidmann, M. S., "Propellant Vaporization as a Design Criterion for Rocket Engine Combustion Chambers," TR-R-67, 1960, NASA.

[17] Williams, F. A., *Combustion Theory*, Addison-Wesley, Reading, Mass., 1965, pp. 56–57.

[18] Dickerson, R. A. and Schuman, M. D., "Rate of Aerodynamic Atomization of Droplets," *Journal of Spacecraft*, Vol. 2, 1965, pp. 99–100.

[19] Barnett, H. C. and Hibbard, R. R., "Properties of Aircraft Fuels," TN 3276, Aug. 1956, NACA.

[20] Bowman, C. T., "Investigation of Nitric Oxide Formation Kinetics in Combustion Processes: The Hydrogen-Oxygen-Nitrogen Reaction," *Combustion Science and Technology*, Vol. 3, 1971, pp. 37–45.

[21] Brinkley, S. R., "Computational Methods in Combustion Calculations," *Combustion Processes, Sect. C; High Speed Aerodynamics and Jet Propulsion*, Vol. 2, edited by B. Lewis, R. N. Pease, and H. S. Taylor, Princeton University Press, Princeton, N.J., 1956.

[22] Brinkley, S. R., "Calculation of the Thermodynamic Properties of Multicomponent Systems and Evaluation of Propellant Performance Parameters," *Proceedings of the First Conference on Kinetics, Equilibrium and Performance of High Temperature Systems*, edited by G. S. Bahn and E. E. Zukoski, The Combustion Inst., 1960, pp. 74–81.

[23] Edelman, R. B. and Fortune, O. F., "A Quasi-Global Chemical Kinetic Model for the Finite Rate Combustion of Hydrocarbon Fuels with Application to Turbulent Burning and Mixing in Hypersonic Engines and Nozzles," AIAA Paper 69-86, New York, 1969.

[24] Baulch, D. L., Drysdale, D. D., Horne, D. G., and Lloyd, A. C., "Critical Evaluation of Rate Data for Homogeneous, Gas Phase Reactions of Interest in High-Temperature Systems," Nos. 1–4, 1968–1969, Dept. of Physical Chemistry, Leeds Univ., England.

[25] Benson, S. W. and Fuens, T., "Mechanism of Atom Recombination by Consecutive Vibrational Deactivations," *Journal of Chemical Physics*, Vol. 36, 1962, pp. 1597–1607.

[26] Camac, M. and Feinberg, R. M., "Formation of NO in Shock-Heated Air," *Eleventh Symposium (International) on Combustion*, The Combustion Inst., 1967, pp. 137–145.

[27] Carnicom, M. L., "Reaction Rates for High Temperature Air," Monograph SCR66-885, 1966, Sandia Labs., Albuquerque, N.Mex.

[28] Lavoie, G. A., Heywood, J. B., and Keck, J. C., "Experimental and Theoretical Study of Nitric Oxide Formation in Internal Combustion Engines," *Combustion Science and Technology*, Vol. 1, 1970, pp. 313–326.